*Articles*

# Comparison of the Structure of the Manganese Complex in the $S_1$ and $S_2$ States of the Photosynthetic $O_2$-Evolving Complex: An X-ray Absorption Spectroscopy Study†

Vittal K. Yachandra,‡ R. D. Guiles,‡,§ Ann E. McDermott,‡,§ James L. Cole,‡,§ R. David Britt,‡,∥ S. L. Dexheimer,‡,∥ Kenneth Sauer,‡,§ and Melvin P. Klein*,‡

*Laboratory of Chemical Biodynamics, Lawrence Berkeley Laboratory, and Departments of Chemistry and Physics, University of California, Berkeley, California 94720*

*Received January 12, 1987; Revised Manuscript Received May 8, 1987*

ABSTRACT: A Mn-containing enzyme complex is involved in the oxidation of $H_2O$ to $O_2$ in algae and higher plants. X-ray absorption spectroscopy is well suited for studying the structure and function of Mn in this enzyme complex. Results of X-ray K-edge and extended X-ray absorption fine structure (EXAFS) studies of Mn in the $S_1$ and $S_2$ states of the photosynthetic $O_2$-evolving complex in photosystem II preparations from spinach are presented in this paper. The $S_2$ state was prepared by illumination at 190 K or by illumination at 277 K in the presence of 3-(3,4-dichlorophenyl)-1,1-dimethylurea (DCMU); these are protocols that limit the photosystem II reaction center to one turnover. Both methods produce an $S_2$ state characterized by a multiline electron paramagnetic resonance (EPR) signal. An additional protocol, illumination at 140 K, produces a state characterized by the $g = 4.1$ EPR signal. We have previously observed a shift to higher energy in the X-ray absorption K-edge energy of Mn upon advancement from the dark-adapted $S_1$ state to the $S_2$ state produced by illumination at 190 K [Goodin, D. B., Yachandra, V. K., Britt, R. D., Sauer, K., & Klein, M. P. (1984) *Biochim. Biophys. Acta 767*, 209–216]. The Mn K-edge spectrum of the 277 K illuminated sample is similar to that produced at 190 K, indicating that the $S_2$ state is similar when produced at 190 or 277 K. A similar edge shape and an edge shift of the same magnitude are seen for the 140 K illuminated sample, establishing that the $S_2$ state can be generated at temperatures as low as 140 K in the absence of the multiline signal. These results indicate that the $g = 4.1$ signal arises from oxidation of the Mn complex and that the structural differences between the species responsible for the $g = 4.1$ signal and the multiline EPR signal are subtle. The salient features of the Mn EXAFS results for the spinach $S_1$ state and for the $S_2$ state generated at 190 K are a Mn neighbor at ~2.70 Å and two shells of N or O at ~1.75 and 2.00 Å, indicative of a $\mu$-oxo-bridged Mn complex. These features are invariant not only for the dark $S_1$ and 190 K illuminated $S_2$ states but also for the $S_2$ state prepared at 277 K, where ligand exchange is considered to be facile. We conclude from the edge and EXAFS studies that the light-induced $S_1$ to $S_2$ transition at 190 K or at 277 K involves a change in the oxidation state of Mn with no EXAFS-detectable change in the coordination of Mn in the $O_2$-evolving complex.

The oxidation of water to molecular oxygen in algae and higher plants involves the stepwise transfer of oxidizing equivalents by the photosystem II (PS II)[1] reaction center. The oxidizing potential produced by photosynthetic charge separation is stored at or near the site of water oxidation in a membrane-bound complex that contains manganese (Sauer, 1980; Amesz, 1983; Dismukes, 1986). Although extensive studies over the past few decades have shown that Mn, $Cl^-$, and $Ca^{2+}$ are involved in this water oxidation reaction, the mechanism of the reaction and the structure of the manganese-containing $O_2$-evolving complex (Mn-OEC) are poorly understood (Govindjee et al., 1985). Studies of $O_2$ evolution using a train of saturating light flashes have given rise to a model in which the oxidizing equivalents produced by the photoreactions of PS II are stored in the Mn-OEC in a stepwise manner until 4 equiv accumulate, at which stage the oxidation of water is completed and $O_2$ is released (Kok et al., 1970). The intermediate states of the Mn-OEC are known as the S states ($S_0$–$S_4$). The chemical identity of the S-state intermediates has been the subject of detailed studies, and

† This work was supported by grants from the National Science Foundation (PCM 82-16127 and PCM 84-16676) and by the Director, Office of Energy Research, Office of Basic Energy Sciences, Division of Biological Energy Conversion and Conservation of the Department of Energy, under Contract DE-AC03-76SF00098. Synchrotron radiation facilities were provided by the Stanford Synchrotron Radiation Laboratory, which is supported by the U.S. Department of Energy, Office of Basic Energy Sciences, and by the NIH Biotechnology Program, Division of Research Resources. This is paper 7 in the series "The State of Manganese in the Photosynthetic Apparatus".

* Correspondence should be addressed to this author.

‡ Laboratory of Chemical Biodynamics, Lawrence Berkeley Laboratory.

§ Department of Chemistry.

∥ Department of Physics.

[1] Abbreviations: Chl, chlorophyll; DCMU, 3-(3,4-dichlorophenyl)-1,1-dimethylurea; DCBQ, 2,6-dichloro-*p*-benzoquinone; EPR, electron paramagnetic resonance; EXAFS, extended X-ray absorption fine structure; MES, 4-morpholineethanesulfonic acid; Mn-OEC, Mn-containing $O_2$-evolving complex; PS II, photosystem II; $P_{680}$, photosystem II reaction center chlorophyll.

0006-2960/87/0426-5974$01.50/0 

evidence implicates the membrane-bound Mn complex.

The first direct spectroscopic evidence for the association of Mn with the S-state intermediates emerged from the observation at low temperature of a complex multiline EPR signal in illuminated spinach chloroplasts (Dismukes & Siderer, 1981; Hansson & Andréasson, 1982), which is similar to that observed in a model binuclear Mn species (Cooper et al., 1978). The flash number dependence of the multiline EPR signal led Dismukes and Siderer (1981) to assign the signal to the $S_2$ state of the $O_2$-evolving complex. The temperature dependence of the light-induced formation and subsequent decay of the signal also indicates that it is correlated with the presence of the $S_2$ state of the $O_2$-evolving complex (Brudvig et al., 1983).

Other evidence for the involvement of Mn in the S states has come from light-induced changes in the UV absorption spectra of PS II preparations. Changes in the absorption spectra have been interpreted to suggest that the $S_1$ to $S_2$ transition corresponds to a Mn(III) to Mn(IV) redox change (Dekker et al., 1984a,b). During one turnover of the PS II reaction center, one electron is transferred from the donor side to the acceptor side of $P_{680}$. However, it has remained controversial whether Mn is oxidized by 1 or 2 equiv during this transition. Lavergne (1986) recently reinterpreted the results from the optical UV difference experiments and suggests that the results are consistent with either 1 or 2 oxidation equiv change for the $S_1$ to $S_2$ transition.

The multiline EPR signal can be produced by illumination at 190 K, by illumination at 277 K in the presence of DCMU, or by flashes at room temperature. Although the multiline signal has been identified with the $S_2$ state (Dismukes & Siderer, 1981), it has been speculated that the state generated at 190 K is different from that generated at 277 K (Hansson & Andréasson, 1982). Ono et al. (1986) showed that, in the absence of $Cl^-$, the multiline signal was not induced by single-flash excitation at 273 K, but upon addition of $Cl^-$ after the flash, the multiline signal developed in the dark. The generation of a modified multiline EPR signal for samples illuminated at 277 K in the presence of 100 mM $NH_4Cl$, together with the failure to observe this modified signal upon illumination at 190 K, suggests that $NH_3$ exchange occurs at the Mn site only at the higher temperature (Beck et al., 1986). Hence, it can be argued in a similar manner that $Cl^-$ exchanges in as a ligand of Mn only when the $S_2$ state is generated at 277 K, or when the sample is warmed to 277 K subsequent to the formation of the $S_2$ state at 190 K. We address the question of $Cl^-$ ligation in the $S_2$ state generated at 190 and 277 K later in this paper.

An EPR signal at $g = 4.1$ has been observed upon illumination at 140 K. Initially, the $g = 4.1$ signal was assigned to an intermediate between the $S_1$ and $S_2$ or the $S_2$ and $S_3$ states (Casey & Sauer, 1984; Zimmermann & Rutherford, 1984). Recently, flash studies by Zimmermann and Rutherford (1986) provided experimental support to indicate that both the multiline EPR signal and the $g = 4.1$ signal arise from different configurations of the light-induced $S_2$ state. On the basis of studies of the temperature dependence of these EPR signals, de Paula et al. (1986) have assigned the multiline signal to a $S = {}^1/_2$ excited state and the $g = 4.1$ signal to a $S = {}^3/_2$ ground state of two different configurations of the Mn complex. Our recent Mn K-edge X-ray absorption studies (Cole et al., 1987) provide confirmation that the $g = 4.1$ signal arises from the Mn complex in the $S_2$ state.

Detailed studies of Mn X-ray K edges provide information about oxidation states and site symmetry, and EXAFS furnishes information about the types of ligands, the Mn to ligand distances, and the coordination number of Mn (Srivastava & Nigam, 1972; Powers, 1982). X-ray spectroscopy is element specific and hence is an appropriate technique if the metalloprotein cannot be isolated to purity. Few other spectroscopic techniques provide such specificity for the structure of the Mn complex in the photosynthetic apparatus. We recently reported light-induced changes in the X-ray Mn K-edge spectra from PS II particles (Goodin et al., 1984a) that provided direct evidence that the membrane-associated Mn atoms participate in the light-driven storage of oxidizing equivalents in the PS II $O_2$-evolving complex. Our earlier EXAFS results (Kirby et al., 1981a), indicative of a binuclear Mn structure in the $O_2$-evolving complex, were obtained from difference EXAFS studies using whole chloroplasts. Our use of PS II subchloroplast preparations that are more homogeneous in Mn content has simplified the data analysis and interpretation of the EXAFS results, without requiring recourse to difficult difference EXAFS studies. Recently, we confirmed the binuclear Mn structure in the dark-adapted $S_1$ state using $O_2$-evolving PS II preparations (Yachandra et al., 1986b).

Our main objective in this paper is to determine the ligand atoms that are coordinated to Mn, the Mn–ligand distances, and the oxidation state of Mn in the $S_1$ state and $S_2$ states. The $S_2$ states were produced by three different protocols: (a) illumination at 190 K, which is characterized by the multiline EPR signal, (b) illumination at 277 K in the presence of DCMU, which is also characterized by the multiline EPR signal, and (c) illumination at 140 K, which is characterized by an EPR signal at $g = 4.1$. Related issues that are addressed in this paper are the question of $Cl^-$ ligation to Mn in the $S_1$ or $S_2$ states and the structural differences between the Mn species giving rise to the $g = 4.1$ or the multiline EPR signal. The edge results demonstrate the similarity between the $S_2$ states generated at the three different temperatures. The EXAFS results show that the $\mu$-oxo-bridged binuclear Mn structure is preserved during the $S_1$ to $S_2$ transition. A scheme for the $S_1$ to $S_2$ state transition is proposed.

## Materials and Methods

Preparation of $O_2$-evolving PS II subchloroplast membranes from market spinach was accomplished by a modification of two different Triton X-100 fractionation procedures (Kuwabara & Murata, 1982; Berthold et al., 1981) and is described in detail elsewhere (Yachandra et al., 1986b). The samples for X-ray absorption studies were about 20–30 mg of Chl/mL and contained approximately 30% glycerol, which is a cryoprotectant. The Mn concentration as measured by atomic absorption spectroscopy was 5 ± 1 Mn atoms per 260 Chl molecules. $O_2$ evolution rates of 300–400 $\mu$mol of $O_2$ (mg Chl)$^{-1}$ h$^{-1}$ were measured in a suspension buffer containing 50 mM MES (pH 6.0), 10 mM NaCl, 5 mM $MgCl_2$, 500 $\mu$M DCBQ, 1 mM $K_3Fe(CN)_6$, and 1 mM $K_4Fe(CN)_6$.

Samples were prepared in the $S_1$ state by incubation in the dark for 2 h at 4 °C (Velthuys & Visser, 1975; Vermaas et al., 1984; Hanssum et al., 1985). The other samples were initially dark adapted and then were equilibrated at 140, 190, or 277 K in a NMR temperature controller and illuminated with a 400-W tungsten lamp through a 5-cm water filter. The samples were then frozen in liquid $N_2$. The 277 K illuminated samples contained DCMU in tenfold excess of the concentration of reaction centers. A stock solution of DCMU was prepared in ethanol, and the final concentration of ethanol in the PS II samples was <1% by volume. The production of the $S_2$ state by illumination at 190 K or at 277 K was monitored by observing the characteristic multiline EPR signal at

8 K. The 140 K illuminated samples were monitored by observing the $g = 4.1$ EPR signal (about 25% of the maximal multiline signal was also induced upon illumination at 140 K).

To ensure the functional and structural integrity of the samples, we monitored the EPR spectra using a Varian E-109 spectrometer before and after X-ray exposure. Spectra were taken at 8 K by using an Air Products liquid He cryostat at a microwave frequency of 9.21 GHz with 100-kHz field modulation. No multiline EPR signal characteristic of the $S_2$ state was observed in the $S_1$ samples before or after X-ray exposure. The amplutide of the multiline EPR signal of the 190 K illuminated sample and of the 277 K illuminated sample decreased by 10–20% after X-ray exposure. A similar decrease in amplitude was seen for the $g = 4.1$ signal for the 140 K illuminated sample. In addition, the $O_2$ evolution activity was assayed before and after X-ray exposure; only small changes (<10%) were observed, ensuring that radiation damage to the functional $O_2$-evolving centers was not significant.

The samples were mounted in Lucite sample holders with a sample area of 2 mm × 3 cm to match the X-ray beam dimensions. The size of the sample holders was so chosen that they could also be inserted into an Air Products Helitran cryostat for monitoring of the EPR spectrum of the sample. Dark adaptation, illumination, EPR, and X-ray measurements were carried out directly in these sample holders. The samples were inserted into a temperature-regulated cryostat in darkness and maintained at 150–190 K for the duration of the X-ray absorption measurements. It has been determined that radiation damage is minimal at temperatures below 190 K. The cryostat, fabricated in our laboratory, consisted of a sample chamber insulated by two layers of Kapton (Du Pont). The sample temperature was regulated by controlling the flow of cooled liquid $N_2$ boil-off. Dry $N_2$ gas was circulated through the space between the layers of Kapton to inhibit frost formation, and air blowers were used to prevent water condensation on the outside of the cryostat.

X-ray absorption edge spectra and EXAFS spectra were collected at the Stanford Synchrotron Radiation Laboratory, Stanford, CA, on wiggler beam lines IV-1 and VI-2 using Si⟨111⟩ or Si⟨400⟩ double-crystal monochromators, respectively, during dedicated operation of the SPEAR storage ring, which provided 20–80-mA electron beams at 3.0 GeV. X-ray absorption spectra were measured in the fluorescence mode (Jaklevic et al., 1977) by using a plastic scintillation array similar to that described by Powers et al. (1981), equipped with Cr filters and a Soller slit assembly to select for Mn fluorescence (Stern & Heald, 1979). Energy calibration was maintained by simultaneous measurement of the strong, narrow pre-edge feature of $KMnO_4$ at 6543.3 eV (Goodin et al., 1979). The uncertainty in our edge energy measurements is ±0.1 eV.

The data were analyzed as described in detail elsewhere (Kirby, 1981; Goodin, 1983). Only a brief summary will be presented here. Before explaining our analysis procedure, it is useful to describe the basic equation for EXAFS modulations. The EXAFS modulation of the absorption $\chi(k)$ is given by the equation:

$$\chi(k) = \frac{\mu(k) - \mu_s(k)}{\mu_0(k)} = \sum_i \frac{N_i |f_i(k,\pi)|}{kR_i^2} e^{-2R_i/\lambda(k)} e^{-2\sigma^2(k)k^2} \sin [2kR_i + \alpha_i(k)]$$

where $\mu(k)$ is the experimentally determined X-ray absorption, $\mu_s(k)$ is the smooth background in the absorption, and $\mu_0(k)$ is the free-atom X-ray absorption. $N_i$ is the number of the $i$th type of backscattering atoms at distance $R_i$, $\lambda(k)$ is the photoelectron mean free path, $f_i(k,\pi)$ is the backscattering amplitude of the $i$th atom [$f_i(k,\pi)$ is $\sim Z/k^2$, for $k > 4$ Å$^{-1}$; $Z$ is the atomic number of the backscattering atom], $\sigma^2(k)$ is the Debye–Waller factor describing the mean square deviation in $R_i$ from thermal and static disorder, $\alpha_i$ is the $k$-dependent phase shift of the photoelectron caused by the potentials of both the absorbing and the backscattering atom, and $k$ is the magnitude of the photoelectron wave vector given by

$$k = \frac{[2m_e(E - E_0)]^{1/2}}{\hbar}$$

where $m_e$ is the electron mass, $E$ is the X-ray photon energy, and $E_0$ is the edge energy (Sayers et al., 1971; Eisenberger & Kincaid, 1978).

For EXAFS analysis, many single scans were added after they were examined for satisfactory signal-to-noise ratio, edge energy registration, and absence of anomalies. Monochromator settings were converted to X-ray energy, and a linear background that set absorption prior to the edge to zero was subtracted from the averaged data. The EXAFS modulation $\chi(k)$ was extracted from the data by subtracting a cubic spline fit to remove the isolated atomic and low-frequency background contribution $\mu_s(k)$ and dividing by the free-atom absorption $\mu_0(k)$. The modulation was normalized to one absorbing atom by the magnitude of the edge. Generally, $\chi(k)$ is multiplied by $k^3$ to compensate for the $1/k^3$ dependence of $\chi(k)$. However, this also increases the noise of the data at higher energies. Because we have a very dilute system (Mn concentration of 500–800 μM) and the signal-to-noise ratio is relatively small, we chose to multiply our data by $k^1$. Fourier transformation of the background-subtracted data produces a radial distribution of photoelectron backscattering as a function of apparent distance $R' = R + \alpha(k)/2$, where $R$ is the true distance from the absorbing atom and $\alpha(k)$ is the phase shift of the absorber–scatterer pair due to their respective potentials (Ashley & Doniach, 1975; Stern, 1974). A window function is applied to isolate the $R'$-space Fourier peaks prior to back-transformation to $k$ space. The back-transformed data were then fit by the Teo–Lee method (Teo & Lee, 1979), which uses theoretical values for the amplitude and phase functions. The values of the average distance, $R$, the number of scattering atoms, $N$, at distance $R$, the Debye–Waller factor, $\sigma$, and the threshold energy, $E_0$, are simultaneously fit with a nonlinear least-squares fitting program. This Fourier filtering method is used to remove the residual low-frequency background and high-frequency noise, thereby greatly improving the precision of the fits.

## Results

Figure 1 shows the representative EPR spectra of PS II samples from spinach in the dark-adapted $S_1$ state and those obtained upon illumination at 140 or 190 K, or at 277 K in the presence of DCMU. The spectrum obtained by illumination at 140 K shows the characteristic $g = 4.1$ signal. Some multiline signal is also evident, and we estimate it to be 25% of that of the 190 K illuminated $S_2$ sample. The kinetics of electron transfer between the quinone acceptors $Q_A$ and $Q_B$ below 190 K limits the PS II reaction center to a one-electron turnover (Joliot, 1974), and one electron is transferred from the donor to the acceptor side of $P_{680}$. The S state generated by illumination at 190 K exhibits the multiline EPR signal, which is a well-characterized spectroscopic signature of the Mn complex in the $S_2$ state (Dismukes & Siderer, 1981; Hansson & Andrêasson, 1982). The EPR spectra observed by illumination at 277 K in the presence of DCMU, which

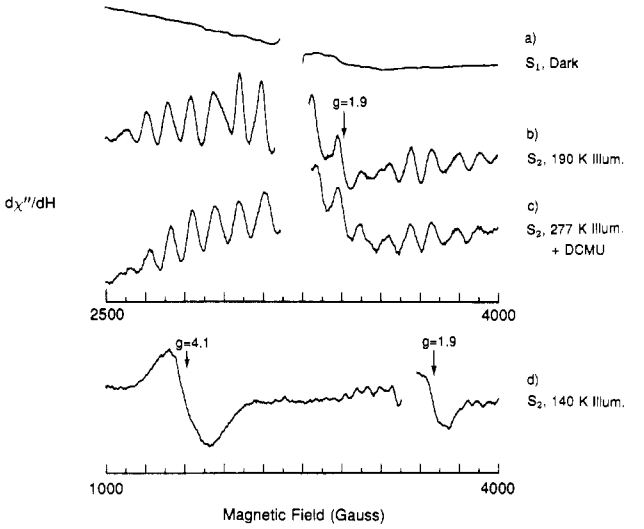


FIGURE 1: EPR spectra of PS II samples from spinach in the (a) dark-adapted $S_1$ state, (b) 190 K illuminated minus dark state, (c) DCMU sample, 277 K illuminated minus dark state, and (d) 140 K illuminated minus dark state. The three light-induced EPR spectra were normalized to the amplitude of the EPR signal of the acceptor $Q_A$ at $g = 1.9$. The EPR spectra were recorded at 8 K by using 50-mW microwave power at 9.21 GHz with 100-kHz field modulation of 32 G; scan time, 4 min; time constant, 0.25 s; and receiver gain, 500. The illumination protocols are described in the text.

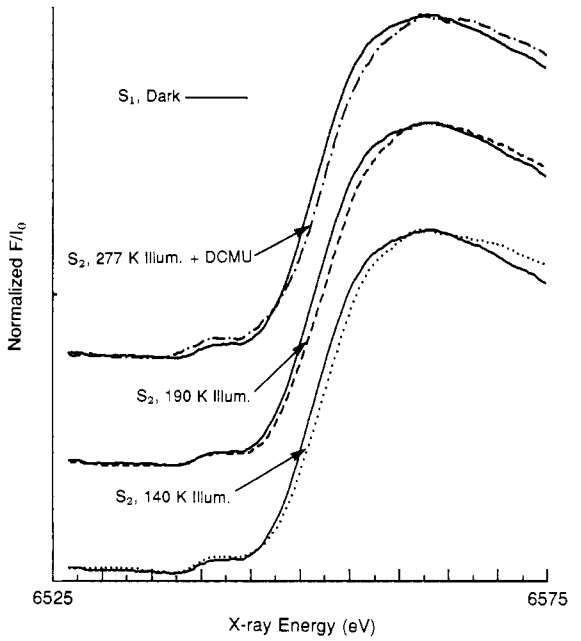


FIGURE 2: X-ray absorption Mn K-edge spectra of spinach PS II samples produced by illumination at 140 (···) or 190 K (- - -) or at 277 K in the presence of DCMU (-·-). The spectrum of the $S_1$ state (—) is overlayed in each case for comparison. The spectra are the sum of two to four scans (3 s/point) and are smoothed by using a second-order polynomial sliding fit (3 eV per fit). The small pre-edge feature at ~6543 eV is due to the 1s–3d bound-state transition. The variation in the size of the pre-edge is within the noise level of the unsmoothed spectra. The K-edge inflection energy for the $S_1$ state is at 6551.3 eV, and that for the 140, 190, and 277 K illuminated samples is at ~6552.5 eV. The K-energy shifts from the dark-adapted $S_1$ state to the illuminated state indicate an oxidation of Mn in the OEC. The edge inflection energies are presented in Table I.

binds at the $Q_B$ binding site and also limits the PS II reaction center to one turnover, is similar to that obtained by 190 K illumination.

The Mn K-edge spectra of samples prepared in the dark-adapted $S_1$ state and of samples illuminated at 140 or 190 K or at 277 K in the presence of DCMU are shown in Figure

Table I: Mn K-Edge Inflection Point Energies for Spinach PS II Samples in the Dark-Adapted and Light-Induced States

| sample | Mn K-edge inflection energies[a] (eV) |
|---|---|
| dark-adapted $S_1$ | 6551.3 |
| 190 K illuminated $S_2$ | 6552.2<br>6552.7 |
| 140 K illuminated, $g = 4.1$ | 6552.6 |
| 277 K illuminated, DCMU | 6552.3 |

[a] The inflection points were obtained from the derivative of a second-order polynomial sliding fit (10 eV per fit) to the edge spectra. The uncertainty in the inflection point energy is ±0.1 eV.

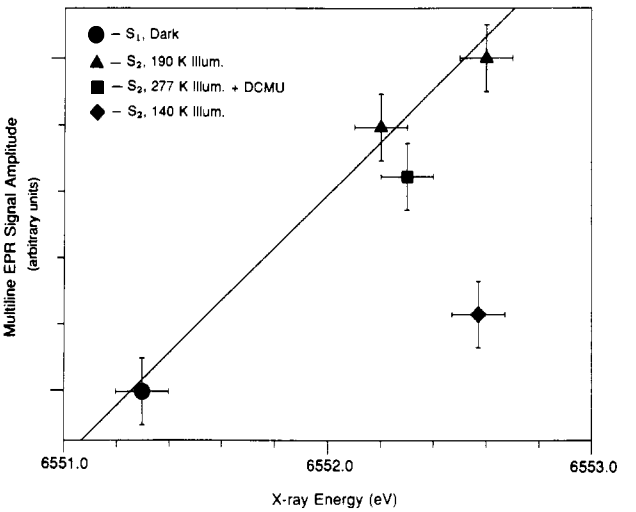


FIGURE 3: Correlation plot of Mn K-edge inflection energies with multiline EPR signal amplitudes for the PS II samples in the dark-adapted and 140, 190, and 277 K illuminated samples. The amplitudes of the multiline signal were taken as the average peak-to-peak height of five lines downfield from $g = 2.0$. The line is a least-squares fit to points from the dark-adapted and 190 K illuminated samples. A line can be drawn through points from the dark-adapted and 190 and 277 K illuminated samples. The 140 K illuminated sample does not fall on the correlation line. The edge positions of all the illuminated samples are in a domain of energies around 6552 eV.

2. The Mn K-edge inflection point of the $S_1$ sample occurs at 6551.3 eV. A shift in the inflection point to higher energy (0.9–1.4 eV) is observed on illuminating the PS II samples at 140 or 190 K, or at 277 K with DCMU present. A very distinct pre-edge transition is seen at ~6543 eV for both the dark and illuminated samples, and the ratio of the amplitude of the pre-edge transition to the amplitude of the K edge ranges from 1:19 to 1:28 for the various samples. The variation in this amplitude ratio among the samples is within the uncertainty due to the signal-to-noise ratio of the spectra. The Mn K-edge inflection energies of the dark-adapted and illuminated samples are summarized in Table I.

Figure 3 shows a plot of the amplitude of the multiline EPR signal vs. the Mn K-edge inflection energy. The amplitudes of the multiline signal were normalized to the chlorophyll content of the samples. As we demonstrated earlier (Goodin et al., 1984a,b), the edge inflection points for the dark-adapted $S_1$ state and the 190 K illuminated samples are well correlated with the observed multiline EPR signal intensities. The K-edge inflection point of the sample illuminated at 277 K in the presence of DCMU is also well correlated with the amplitude of the multiline EPR signal. The inflection point of the sample illuminated at 140 K is not correlated with the amplitude of the multiline signal, but the inflection point energy of this sample is in the domain of energies observed for the 190 K illuminated samples at about 6552.5 eV. However, in this

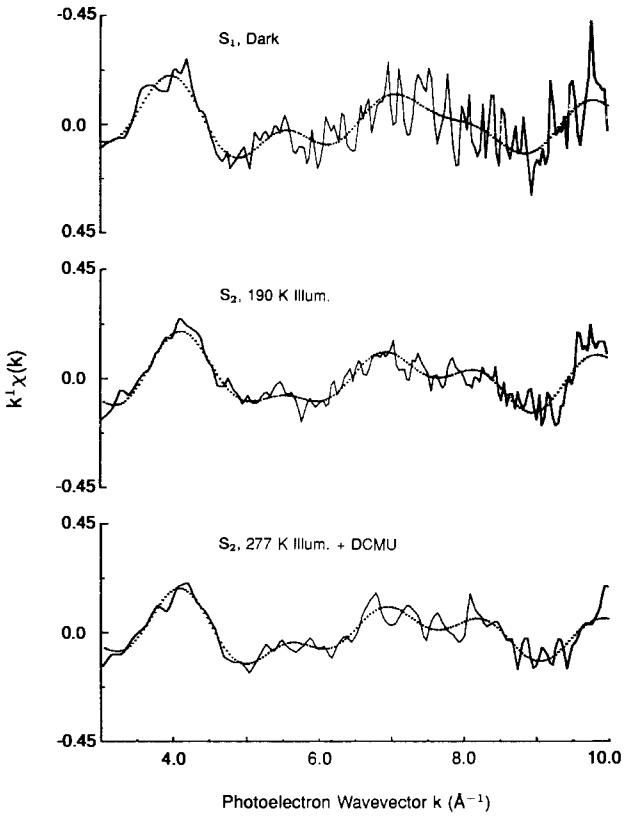


FIGURE 4: Background-subtracted (cubic spline) $k^1$-weighted Mn EXAFS data $\chi(k)$ plotted as a function of the photoelectron wave vector, $k$. The data are normalized to unit edge rise by extrapolation of the smooth free-atom background of PS II samples in the dark-adapted $S_1$ state, 190 K illuminated $S_2$ state, and 277 K illuminated $S_2$ state. The dotted lines are the Fourier-filtered EXAFS data. The modulations are complicated, indicating that there is more than one sinusoidal EXAFS component in the spectra, which is suggestive of a coordination sphere of Mn consisting of different atoms, the same ligand atoms at different distances, or both.

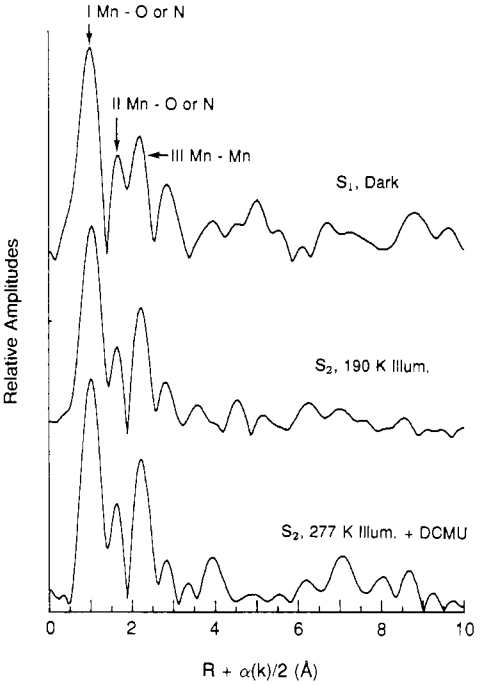


FIGURE 5: Fourier transforms of the $k^1$-weighted Mn EXAFS data from the spinach $S_1$ state and the $S_2$ states produced by illumination at 190 K or at 277 K in the presence of DCMU. Note that the Fourier peaks are at smaller values than the real distances $R$ by about 0.5 Å. The peaks labeled I and II are characteristic of bridging and terminal N or O ligands, respectively, and peak III is due to a neighboring Mn atom; the distances are typical for $\mu$-oxo-bridged binuclear Mn clusters. The peak labeled I fits best to N or O ligand atoms at 1.75 Å, peak II fits to N or O ligand atoms at 2.00 Å, and peak III fits to Mn at 2.70 Å. We estimate the uncertainty in distances to be ±0.03 Å for the Mn–Mn distance and ±0.05 Å for the terminal and bridging ligand distances. The fits were performed by using theoretical phase and amplitude functions by the Teo-Lee method (Teo & Lee, 1979). The differences in the amplitude of the first Fourier peak are due to background removal difficulties and are not significant. The peaks at $R + \alpha(k)/2 > 3.5$ Å are within the level of noise.

sample an EPR signal at $g = 4.1$ is observed, in addition to ~25% of the control multiline EPR signal amplitude.

Figure 4 shows the $k^1$-multiplied, background-subtracted EXAFS spectra of samples in the dark-adapted $S_1$ state and in the 190 K illuminated and 277 K illuminated $S_2$ states. It is evident that the EXAFS modulations are complicated and are characterized by contributions from more than one sinusoidal oscillation, which is indicative of a coordination sphere about Mn consisting of different ligand atoms, the same ligand atom at more than one distance, or both. It is also clear from Figure 4 that the spectra of the $S_1$, 190 K illuminated $S_2$, and 277 K illuminated $S_2$ samples are very similar. The Fourier-filtered curve is overlayed on the EXAFS data in each case.

The contribution of various scattering shells to the EXAFS spectrum becomes more evident in the Fourier transform of the $k$-space data, which produces a radial distribution of the photoelectron backscattering, as illustrated in Figure 5. The Fourier peaks appear at similar positions in the dark-adapted $S_1$ sample and in the $S_2$ samples produced by illumination at 190 K or at 277 K in the presence of DCMU. The peak labeled I at $R' = R + \alpha(k)/2 \sim 1.1$ Å is due to the nearest-neighbor atoms (first shell). The second peak labeled II occurs at $R' \sim 1.6$ Å and is from a second shell of ligands. The third Fourier peak (III) occurs at $R' \sim 2.2$ Å. The Fourier peak labeled III increases in amplitude as a function of $k$ weighting relative to the first and second peaks (not shown). This behavior is indicative that the scattering contribution is from a transition metal, which in this case is probably Mn (Kirby, 1981). Note that the real distances $R$ are larger than $R'$. Small differences are seen among the amplitudes of the Fourier peaks from the dark-adapted, 190 K illuminated, and 277 K illuminated samples, especially in the first two peaks. The differences in the amplitude of the first peak are probably due to background removal difficulties. The amplitude differences in the second shell may reflect real changes, but the signal-to-noise ratio limitations in the spectra of the three samples preclude a more definite statement.

The Fourier-filtered data were fit to phase and amplitude functions obtained from theoretical calculations that have been compared with experimentally determined values. The best fit parameters indicate that each Mn atom is coordinated to about 2 O or N ligand atoms at 1.75 Å, to about 3 N or O ligand atoms at a distance of 2.00 Å, and to 0.5–2 Mn atoms at a distance of 2.70 Å. The uncertainty in $R$ is ±0.05 Å for the N or O distances and ±0.03 Å for the Mn distance. Significant correlations exist between $N$ and $\sigma$, making the error in $N$ typically 20%; it can often be as high as 50% (Eisenberger & Lengeler, 1980). The results are summarized in Table II. Broad background oscillations contribute significantly to the amplitude of the first Fourier peak, making an estimation of the coordination number difficult. Similar problems are encountered with the estimation of the coordination number from the second shell because it often cannot be resolved from the first shell. We are able to specify a range of uncertainty for the third shell because it is clearly isolated, and it is not so sensitive to broad oscillations and related background removal difficulties. The range of uncertainty will

Table II: Parameters Extracted from Mn EXAFS Data from PS II Particles in the Dark-Adapted $S_1$ State and Light-Induced $S_2$ State Generated at 190 or 277 K Illumination, by the Teo–Lee Method (Teo & Lee, 1979)[a,b,c,d]

| | distance $R$ (Å) | | |
|---|---|---|---|
| | $S_1$ | $S_2$, 190 K illumination | $S_2$, 277 K illumination |
| I, Mn–O or N bridging ligand | 1.75 | 1.76 | 1.76 |
| II, Mn–O or N terminal ligand | 2.00 | 1.98 | 1.99 |
| III, Mn–Mn | 2.70 | 2.72 | 2.72 |

[a] $R$ is the distance from Mn to the various scattering atoms. The uncertainty is ±0.05 Å for the bridging and terminal ligand distances and is ±0.03 Å for the Mn–Mn distance. [b] The coordination number $N$ for the first shell is ~2, for the second shell $N$ is ~3, and is 0.5–2.0 for the third shell. [c] The Debye–Waller factor $\sigma$ used in the simulations was fixed at a value of 0.022 Å. [d] $\Delta E_0$ used in the simulations was allowed to vary from −20 to +20 eV from $E_0$, which was the energy at the top of the edge. The difference in $\Delta E_0$ for the three shells was not allowed to exceed 17 eV.

be narrowed in the future as more model inorganic compounds become available, providing better scaling factors for determining the coordination numbers.

## Discussion

*X-ray Absorption Edge Studies.* The position of the K-edge inflection is a good indicator of the oxidation state of the metal in a complex, and a correlation of the K-edge inflection energy of Mn with the oxidation state of Mn was presented in an earlier study (Kirby et al., 1981b). However, it should be noted that the position of the edge inflection is also modulated by the nature of the ligands, which gives rise to overlapping energy ranges for different oxidation states. The Mn K-edge inflection of the $S_1$ samples occurs at about 6551.3 eV, which is in the range of K edges of Mn(III) complexes (R. D. Guiles, unpublished observations; Kirby et al., 1981b). The K-edge inflection of the illuminated samples shifts to higher energy and occurs at ~6552.5 eV, which is between that observed for Mn(III) and Mn(IV) complexes. These K-edge positions are higher and the K-edge shifts on illumination are smaller than the values we reported earlier (Goodin et al., 1984a). We believe that this discrepancy is due to the presence of some adventitiously bound Mn(II) in the samples used in our earlier work; the presence of Mn(II) would lower the inflection point, and different amounts of Mn(II) in $S_1$ and $S_2$ samples would change the magnitude of the K-edge shift. Repeated freezing and thawing procedures followed in the earlier experiments are now known to release some Mn(II), which exhibits a characteristic six-line EPR signal. Care was taken in our present experiments to avoid such freeze–thaw procedures; the samples used in our present study contain <10% Mn(II) as monitored by EPR (compared to total Mn content).

The Mn K-edge shift of 0.9–1.4 eV that is observed between the dark-adapted and the light-induced samples is similar to changes that are observed upon one-electron oxidation of binuclear Mn model systems (Kirby et al., 1981b; R. D. Guiles, unpublished observations). For example, a shift of ~1 eV is observed between the edge positions of isomorphous $Mn^{III}Mn^{III}$ and $Mn^{III}Mn^{IV}$ binuclear complexes with mixed N and O ligands. However, it is not possible to rule out a two-electron change in the $S_1$ to $S_2$ transition only on the basis of the magnitude of the edge shift (Goodin et al., 1984a). We have shown that no major changes are evident in the EXAFS spectra of the dark-adapted and light-induced states, indicating that the Mn structures in the two states are indistinguishable by EXAFS criteria. EXAFS results from bis($\mu$-oxo)-bridged $Mn^{III}Mn^{IV}$ and $Mn^{IV}Mn^{IV}$ model compounds (Kirby et al., 1981a) showed that the complexes have similar structures in the two available oxidation states. Because no major structural change associated with the $S_1$ to $S_2$ transition is apparent, we conclude that the observed edge shifts are predominantly due to the oxidation-state change of Mn in the complex.

The Mn K-edge spectra of the PS II samples show a 1s–3d pre-edge transition at ~6543 eV. The intensity of this transition is indicative of a noncentrosymmetric ligand environment for Mn (Shulman et al., 1976; Roe et al., 1984). A pre-edge feature of similar intensity has also been shown to be present in exchange-coupled binuclear iron complexes (Roe et al., 1984). The edge spectra also show distinct shoulders on the rising edge of the inflection that are more evident in the first derivative spectra (not shown); a comparison with model multinuclear Mn complexes is under way and will be the subject of a future publication (R. D. Guiles, unpublished observations).

Our present results show that the Mn K edge of dark-adapted samples shifts to higher energy upon illumination at 140 K, producing a state characterized by the presence of the $g = 4.1$ EPR signal and the absence of the multiline EPR signal. The Mn K-edge data conclusively show that, following illumination, even at 140 K, Mn is oxidized relative to the Mn in the dark-adapted state. We conclude that it is possible to advance to the $S_2$ state at 140 K. These results show that the multiline EPR signal is only one indicator of the formation of the light-induced $S_2$ state and that it is not always observed. Recently, Ono et al. (1986) showed that the $S_2$ state, as defined by the storage of oxidizing equivalents, can be generated in chloride-depleted preparations without producing the multiline EPR signal. Earlier studies had shown that the $g = 4.1$ signal generated by illumination at 140 K decreases in amplitude on warming to 190 K with a concurrent increase in the amplitude of the multiline EPR signal (Casey & Sauer, 1984). Recently, Zimmermann and Rutherford (1986) have shown from flash studies that the amplitude of the $g = 4.1$ signal oscillates with a period of four, showing a maximum on the first and fifth flashes. The pattern is similar to that observed for the multiline signal; on the basis of this observation, the $g = 4.1$ signal has been assigned to a different spin state that is preferably observed in another configuration of the $S_2$ state. This is consistent with the model proposed by de Paula et al. (1986) that the $g = 4.1$ signal and the multiline signal are from two different spin states which are preferentially populated in the two different configurations of the Mn complex in the light-induced $S_2$ state. The Mn K-edge data do not provide any information about the specific spin states proposed by de Paula et al. (1986). However, the similarity of the edge spectrum of the 140 K illuminated sample to the spectrum of the 190 K illuminated sample indicates that the structural differences between the two configurations must be subtle.

The Mn K-edge inflection point also shifts to higher energy for the sample illuminated at 277 K in the presence of DCMU, which restricts the PS II reaction center to one turnover. The edge shift is correlated with the amplitude of the multiline signal (Figure 3). The position of the inflection, the shape of the spectrum, and the shift in energy relative to the dark sample are similar to those observed for the 190 or 140 K illuminated samples. The shape of the edge spectrum is a sensitive indicator of the coordination structure of the metal as has been shown in many studies (Srivastava & Nigam, 1972). The lack of any major change in shape and position of the edge, or in the 1s–3d pre-edge transition, indicates that the essential structure of the Mn complex is unchanged between samples illuminated at 140, 190, and 277 K. This

question is further addressed by the EXAFS studies, which provide more detailed information about the coordinating ligands of Mn.

*EXAFS Studies.* The salient features of the Mn EXAFS spectra of the light-induced $S_2$ state produced by illumination at 190 K and characterized by the multiline signal are essentially identical with those observed for the dark-adapted $S_1$ state. Although we do not yet have EXAFS results for the 140 K illuminated sample, we think it is unlikely that there is a major change in coordination of Mn at this temperature, in light of our results for the 190 and 277 K illuminated samples, which do not exhibit any major coordination changes. The EXAFS and edge results from samples prepared in the $S_1$ and light-induced $S_2$ states support the model that the light-induced $S_1$ to $S_2$ transition involves a change in the oxidation state of Mn with essentially no change in the coordination of Mn.

The EXAFS results for both the $S_1$ and $S_2$ states are consistent with a binuclear Mn structure with a Mn–Mn distance of 2.70 Å, with each Mn coordinated to approximately three N or O terminal ligands at 2.00 Å and approximately two N or O bridging ligands at a distance of 1.75 Å. These coordination numbers and bond lengths resemble the published crystal structure parameters for the bis($\mu$-oxo)tetrakis(2,2′-bipyridine)dimanganese(III,IV) perchlorate (Plaksin et al., 1972).

It is generally agreed that there are about 4 Mn atoms/PS II reaction center. EXAFS data provide a composite measure of the coordination of all of the Mn atoms in the system, and our results are suggestive that each Mn atom is associated with 0.5–2.0 Mn atoms at ~2.7 Å. Two of the likely possibilities that are consistent with our data are as follows: (1) two equivalent binuclear complexes separated from one another by >3 Å, which would give an average Mn coordination of 1.0 per Mn atom, or (2) one binuclear complex with 2 other Mn atoms incorporated as monomers at distances >3 Å from the binuclear complex; this would arrive at a Mn coordination of 0.5, which is within the limits of the uncertainty of our measurements and analytical procedures. Recently, we have identified a fourth peak in the Fourier transform of the EXAFS spectrum at $R > 3$ Å that can be assigned to a Mn atom, lending support to either of the above models (Guiles et al., 1987). A symmetric tetranuclear Mn structure with equidistant Mn centers would give a Mn coordination number of 3.0, which is beyond the limits of the error inherent in our measurements.

A related question has been the proposal for $Cl^-$ coordination to Mn (Sandusky & Yocum, 1983; Critchley, 1985; Kelley & Izawa, 1978) in the dark-adapted and/or in the light-induced states (Preston & Pace, 1985). Typical Mn(III)–Cl distances are in the range 2.3–2.5 Å in Schiff base and porphyrin complexes (Boucher & Day, 1977; Tulinsky & Chen, 1977; Pecoraro & Butler, 1986). $Cl^-$ ligands at this distance would give rise to a Fourier peak at $R' \sim 2.0$ Å. The Fourier transforms shown in Figure 5 are devoid of any such feature. Forcing 1 Cl scatterer per 4 Mn atoms at a distance of 2.3–2.5 Å into our simulations resulted in no change in the quality of the fit for the spectra of the dark-adapted and of the 190 or 277 K illuminated samples. Thus, based only on EXAFS results, it is not possible to rule out the presence of 1 Cl scatterer per 4 Mn atoms. However, our recently published high-resolution multiline EPR results (Yachandra et al., 1986a) show that no significant differences are observed in the EPR fine structure, a multiplet of four to six lines with 10–15-G spacing, between the $Cl^-$- and $Br^-$-containing samples, suggesting that the halide is not a ligand of Mn. The EPR studies along with the EXAFS studies are indicative that $Cl^-$ is not in the first coordination shell of Mn in the dark-adapted or in the light-induced states produced by illumination at 190 or 277 K. The similarity of the EXAFS spectra of the 190 and 277 K illuminated samples, along with the identical K-edge spectra of these samples, rules out any major change in the coordination sphere of Mn at 277 K that can be detected by X-ray absorption spectroscopy. Our current EXAFS studies are addressing the possible ligation of halide by using bromide-substituted samples, because bromine is a better X-ray scatterer than is chlorine.

*The $S_1$ to $S_2$ Transition of the $O_2$-Evolving Complex.* From our studies we conclude the following: (1) The oxidation state of Mn increases by 1 or 2 equiv/four equiv of Mn atoms in the $S_1$ to $S_2$ transition. (2) The oxo-bridged binuclear Mn structure with N or O terminal ligands is unchanged by the $S_1$ to $S_2$ transition. (3) The structure of the Mn complex is essentially the same in the $S_2$ states generated at 190 K and at 277 K.

On the basis of the EPR hyperfine structure of the multiline signal and its similarity to the bipyridyl binuclear Mn complex, Dismukes et al. (1982) proposed a weakly exchange coupled $Mn^{III}Mn^{IV}$ binuclear or a $Mn^{III}Mn^{III}Mn^{III}Mn^{IV}$ tetranuclear structure to be present in the light-induced $S_2$ state. Hansson and Andréasson (1982) and Andréasson et al. (1983) find that $Mn^{II}Mn^{III}$ is in better agreement with their data. More recently, the temperature dependence of the multiline signal and the assignment of the $g = 4.1$ signal to an $S = {}^3/_2$ ground state of the $S_2$ state led Brudvig and Crabtree (1986) to propose a tetranuclear cubane-like structure.

Combining the studies mentioned above with our edge and EXAFS data, we have arrived at a model for the light-induced $S_1$ to $S_2$ transition. Our edge and EXAFS data are consistent with a $Mn^{II}Mn^{III}$ or $Mn^{III}Mn^{III}$ $\mu$-oxo-bridged binuclear complex for the $S_1$ state. However, a mixed-valence $Mn^{II}Mn^{III}$ complex is expected to be EPR-active, and Mabad et al. (1985) have shown that a $Mn^{II}Mn^{III}$ model compound exhibits a characteristic 16-line EPR spectrum. Studies with PS II samples in the $S_1$ state have not yet exhibited such an EPR spectrum, suggesting that the $Mn^{III}Mn^{III}$ is more likely to be present in the $S_1$ state. On illumination, the Mn complex in photosystem II is oxidized to an EPR-active $Mn^{III}Mn^{IV}$ $\mu$-oxo-bridged binuclear complex. The transition from the $S_1$ to $S_2$ state does not involve any major changes that are detectable by EXAFS in the coordination sphere of Mn. The two other Mn atoms present in the PS II complex are both in either the +3 or +4 oxidation state. These two Mn atoms could be arranged in two different ways: (1) a second oxo-bridged binuclear cluster 3 Å or more away from the first one or (2) two mononuclear Mn species 3 Å or more away from the oxo-bridged binuclear cluster.

## ACKNOWLEDGMENTS

We are grateful to Dr. David Goodin for helpful discussions concerning X-ray fluorescence detection. We thank Richard Storrs for help with data collection and Andrew Gewirth for help at Stanford. We also thank the staff at the Stanford Synchrotron Radiation Laboratory for their assistance.

**Registry No.** Mn, 7439-96-5.

## REFERENCES

Amesz, J. (1983) *Biochim. Biophys. Acta 726*, 1–12.

Andréasson, L.-E., Hansson, Ö., & Vänngård, T. (1983) *Chem. Scr. 21*, 71–74.

Ashley, C. A., & Doniach, S. (1975) *Phys. Rev. B: Solid State 11*, 1279–1288.
Beck, W. F., de Paula, J. C., & Brudvig, G. W. (1986) *J. Am. Chem. Soc. 108*, 4018–4022.
Berthold, D. A., Babcock, G. T., & Yocum, C. F. (1981) *FEBS Lett. 134*, 231–234.
Boucher, L. J., & Day, V. W. (1977) *Inorg. Chem. 16*, 1360–1367.
Brudvig, G. W., & Crabtree, R. H. (1986) *Proc. Natl. Acad. Sci. U.S.A. 83*, 4586–4588.
Brudvig, G. W., Casey, J. L., & Sauer, K. (1983) *Biochim. Biophys. Acta 723*, 366–371.
Casey, J. L., & Sauer, K. (1984) *Biochim. Biophys. Acta 767*, 21–28.
Cole, J., Yachandra, V. K., Guiles, R. D., McDermott, A. E., Britt, R. D., Dexheimer, S. L., Sauer, K., & Klein, M. P. (1987) *Biochim. Biophys. Acta 890*, 395–398.
Cooper, S. R., Dismukes, G. C., Klein, M. P., & Calvin, M. (1978) *J. Am. Chem. Soc. 100*, 7248–7252.
Critchley, C. (1985) *Biochim. Biophys. Acta 811*, 33–46.
Dekker, J. P., Van Gorkom, H. J., Brok, M., & Ouwehand, L. (1984a) *Biochim. Biophys. Acta 764*, 301–309.
Dekker, J. P., Van Gorkom, H. J., Wensink, J., & Ouwehand, L. (1984b) *Biochim. Biophys. Acta 767*, 1–9.
de Paula, J. C., Beck, W. F., & Brudvig, G. W. (1986) *J. Am. Chem. Soc. 108*, 4002–4009.
Dismukes, G. C. (1986) *Photochem. Photobiol. 43*, 99–115.
Dismukes G. C., & Siderer, Y. (1981) *Proc. Natl. Acad. Sci. U.S.A. 78*, 274–278.
Dismukes, G. C., Ferris, K., & Watnick, P. (1982) *Photobiochem. Photobiophys. 3*, 243–256.
Eisenberger, P., & Kincaid, B. M. (1978) *Science (Washington, D.C.) 200*, 1441–1447.
Eisenberger, P., & Lengeler, B. (1980) *Phys. Rev. B: Condens. Matter 22*, 3551–3562.
Goodin, D. B. (1983) Ph.D. Dissertation, University of California, Berkeley, CA (Lawrence Berkeley Laboratory Report No. LBL-16901).
Goodin, D. B., Falk, K.-E., Wydrzynski, T., & Klein, M. P. (1979) *Sixth Annual Stanford Synchrotron Radiation Laboratory Users Group Meeting*, SSRL Report No. 79/05, pp 10–11, Stanford University, Stanford, CA.
Goodin, D. B., Yachandra, V. K., Britt, R. D., Sauer, K., & Klein, M. P. (1984a) *Biochim. Biophys. Acta 767*, 209–216.
Goodin, D. B., Yachandra, V. K., Guiles, R. D., Britt, R. D., McDermott, A., Sauer, K., & Klein, M. P. (1984b) in *EXAFS and Near Edge Structure III* (Hodgson, K. O., Hedman, B., & Penner-Hahn, J. E., Eds.) pp 130–135, Springer-Verlag, New York.
Govindjee, Kambara, T., & Coleman, W. (1985) *Photochem. Photobiol. 42*, 187–210.
Guiles, R. D., Yachandra, V. K., McDermott, A. E., Britt, R. D., Dexheimer, S. L., Sauer, K., & Klein, M. P. (1987) in *Progress in Photosynthesis Research* (Biggins, J., Ed.) Vol. 1, pp 561–564, Nijhoff, Dordrecht.
Hansson, Ö., & Andréasson, L.-E. (1982) *Biochim. Biophys. Acta 679*, 261–268.
Hanssum, B., Dohnt, G., & Renger, G. (1985) *Biochim. Biophys. Acta 806*, 210–220.
Jaklevic, J., Kirby, J., A., Klein, M. P., Robertson, A. S., Brown, G. S., & Eisenberger, P. (1977) *Solid State Commun. 23*, 679–682.
Joliot, A. (1974) *Biochim. Biophys. Acta 357*, 439–448.
Kelley, P. M., & Izawa, S. (1978) *Biochim. Biophys. Acta 502*, 198–210.
Kirby, J. A. (1981) Ph.D. Dissertation, University of California, Berkeley, CA (Lawrence Berkeley Laboratory Report No. LBL-12705).
Kirby, J. A., Robertson, A. S., Smith, J. P., Thompson, A. C., Cooper, S. R. & Klein, M. P. (1981a) *J. Am. Chem. Soc. 103*, 5529–5537.
Kirby, J. A., Goodin, D. B., Wydrzynski, T., Robertson, A. S., & Klein, M. P. (1981b) *J. Am. Chem. Soc. 103*, 5537–5542.
Kok, B., Forbush, B., & McGloin, M. P. (1970) *Photochem. Photobiol. 11*, 457–475.
Kuwabara, T., & Murata, N. (1982) *Plant Cell Physiol. 23*, 533–539.
Lavergne, J. (1986) *Photochem. Photobiol. 43*, 311–317.
Mabad, B., Tuchagues, J.-P., Hwang, Y. T., & Hendrickson, D. N. (1985) *J. Am. Chem. Soc. 107*, 2801–2802.
Ono, T., Zimmermann, J. L., Inoue, Y., & Rutherford, A. W. (1986) *Biochim. Biophys. Acta 851*, 193–201.
Pecoraro, V. L., & Butler, W. M. (1986) *Acta Crystallogr., Sect. C: Cryst. Struct. Commun. C42*, 1151–1154.
Plaksin, P. M., Stoufer, R. C., Mathew, M., & Palenik, G. J. (1972) *J. Am. Chem. Soc. 94*, 2121–2122.
Powers, L. (1982) *Biochim. Biophys. Acta 683*, 1–38.
Powers, L., Chance, B., Ching, Y., & Angiolillo, P. (1981) *Biophys. J. 34*, 465–498.
Preston, C., & Pace, R. J. (1985) *Biochim. Biophys. Acta 810*, 388–391.
Roe, A. L., Schneider, D. J., Mayer, R. J., Pyrz, J. W., Widom, J., & Que, L., Jr. (1984) *J. Am. Chem. Soc. 106*, 1676–1681.
Sandusky, P. O., & Yocum, C. F. (1983) *FEBS Lett. 162*, 339–343.
Sauer, K. (1980) *Acc. Chem. Res. 13*, 249–256.
Sayers, D. E., Stern, E. A., & Lytle, F. W. (1971) *Phys. Rev. Lett. 27*, 1204–1207.
Shulman, R. G., Yafet, Y., Eisenberger, P., & Blumberg, W. E. (1976) *Proc. Natl. Acad. Sci. U.S.A. 73*, 1384–1388.
Srivastava, U. C., & Nigam, H. L. (1972) *Coord. Chem. Rev. 9*, 275–310.
Stern, E. A. (1974) *Phys. Rev. B: Solid State 10*, 3027–3037.
Stern, E. A., & Heald, S. M. (1979) *Rev. Sci. Instrum. 50*, 1579–1582.
Teo, B.-K., & Lee, P. A. (1979) *J. Am. Chem. Soc. 101*, 2815–2832.
Tulinsky, A., & Chen, B. M. L. (1977) *J. Am. Chem. Soc. 99*, 3647–3651.
Velthuys, B. R., & Visser, J. W. M. (1975) *FEBS Lett. 55*, 109–112.
Vermaas, W. F. J., Renger, G., & Dohnt, G. (1984) *Biochim. Biophys. Acta 764*, 194–202.
Yachandra, V. K., Guiles, R. D., Sauer, K., & Klein, M. P. (1986a) *Biochim. Biophys. Acta 850*, 333–342.
Yachandra, V. K., Guiles, R. D., McDermott, A., Britt, R. D., Dexheimer, S. L., Sauer, K., & Klein, M. P. (1986b) *Biochim. Biophys. Acta 850*, 324–332.
Zimmermann, J. L., & Rutherford, A. W. (1984) *Biochim. Biophys. Acta 767*, 160–167.
Zimmermann, J. L., & Rutherford, A. W. (1986) *Biochemistry 25*, 4609–4615.